DFT Modeling of NMR Contact Shift Mechanism in the Ideal $LiNi_2O_4$ Spinel and Application to Thermally Treated Layered $Li_{0.5}NiO_2$

Cédric Chazel, Michel Ménétrier,* Dany Carlier, Laurence Croguennec, and Claude Delmas

ICMCB, CNRS, Université Bordeaux 1, Site de l'ENSCPB, 87 Avenue Schweitzer, 33608 PESSAC Cedex, France

Received February 2, 2007. Revised Manuscript Received April 19, 2007

$LiNi_2O_4$ spinel-type phases were prepared by thermal treatment of electrochemically deintercalated layered $Li_{\sim 0.5}NiO_2$. The phase transformation was followed by ^{7}Li NMR, showing a gradual change of the signal from the layered compound. The characteristic signal of the latter (related to local Li/vacancy and Ni^{3+}/Ni^{4+} ordering) vanishes after heating to 150 °C and is replaced by a new signal showing faster exchange kinetics (originating from Ni^{3+}/Ni^{4+} hopping around Li), which progressively transforms into a broad distribution of signals. Around 200 °C, a set of three positively shifted signals is observed, corresponding to the appearance of the spinel phase as seen from XRD; these signals disappear after heating to 240 °C, corresponding to the beginning of decomposition of the spinel into a disordered $R\bar{3}m$ type phase with oxygen evolution as previously shown by Guilmard et al. (*Chem. Mater.* **2003**, *15*, 4476 and 4484). In an ideal $LiNi_2O_4$ spinel, only one ^{7}Li NMR signal is expected. DFT (GGA) calculations were carried out and show that the mechanism for the electron spin density transfer from NiO_6 octahedra to corner-sharing LiO_4 tetrahedra with close to 120° Ni−O−Li configuration is a delocalization one, although the p orbitals on oxygen do not present ideal orientation, leading to a much weaker transfer compared to cases where both Ni and Li are in octahedral coordination with 180° Ni−O−Li configuration. The complex but well-defined experimental NMR signals consistently observed show that the material is far from the ideal spinel structure. However, it could not be correlated to the actual stoichiometry of the compound. It was therefore tentatively assigned to structural defects resulting from incomplete migration of Ni ions from their site to the Li layer in the pristine compound, such as partial occupation of tetrahedral sites.

Introduction

Li NMR in transition metal oxides used as positive electrode materials for lithium-ion batteries is a fast growing research field, as recently reviewed by Grey and Dupré.[1] It aims both at better understanding the NMR shift mechanisms in this class of compounds, and at bringing some insight to their local structure in terms of defects and on the mechanisms of the redox reactions they undergo upon Li intercalation/deintercalation.

In this area, we have studied Co- and Ni-based compounds for some time.[2−9] Thanks to DFT calculations of the polarized spin density on the Li nucleus, the processes leading to the transfer of electron spin density from a transition metal ion to the Li nucleus could be understood when both Li and the transition metal are octahedrally coordinated by oxygen, which is the case for layered compounds such as the O3 $LiMO_2$ phases built of alternate layers of edge-sharing LiO_6 and MO_6 octahedra.[10] The Li−O−M configuration can either be 180° (corner-sharing octahedra) or 90° (edge-sharing octahedra). When the orbital containing the electron spin can overlap with the Li 2s orbital (either directly or via an oxygen p orbital), a positive electron spin density is transferred (the delocalization mechanism). When no direct overlap is possible with the M orbital carrying the spin, some spin density can still be transferred by delocalization from a fully occupied M orbital, which gets polarized by an electron spin in a higher energy orbital (the polarization mechanism). The interplay of these mechanisms is summarized in Table 1 and is valid in the case of triply degenerate t_{2g} and doubly degenerate e_g* orbitals, i.e., without distortion or the Jahn−Teller effect. Note that, in this paper, the antibonding hybrid metal(3d)−oxygen(2p) orbital with strong metal character is called e_g*, to make a distinction from its bonding e_g counterpart with strong

* Corresponding author. Phone: 33 5 40 00 66 39. Fax: 33 5 40 00 27 61. E-mail: menetrier@icmcb-bordeaux.CNRS.fr.

(1) Grey, C. P.; Dupré, N. *Chem. Rev.* **2004**, *104* (10), 4493−4512.
(2) Chazel, C.; Ménétrier, M.; Croguennec, L.; Delmas, C. *Magn. Reson. Chem.* **2005**, *43*, 849−857.
(3) Levasseur, S.; Ménétrier, M.; Delmas, C. *J. Electrochem. Soc.* **2002**, *149* (12), A1533−1540.
(4) Levasseur, S.; Ménétrier, M.; Delmas, C. *J. Power Sources* **2002**, *112* (2), 419−427.
(5) Levasseur, S.; Ménétrier, M.; Delmas, C. *Chem. Mater.* **2002**, *14*, 3584−3590.
(6) Carlier, D.; Ménétrier, M.; Delmas, C. *J. Mater. Chem.* **2001**, *11*, 594−603.
(7) Levasseur, S.; Ménétrier, M.; Suard, E.; Delmas, C. *Solid State Ionics* **2000**, *128*, 11.
(8) Ménétrier, M.; Saadoune, I.; Levasseur, S.; Delmas, C. *J. Mater. Chem.* **1999**, *9*, 1135−1140.
(9) Marichal, C.; Hirschinger, J.; Granger, P.; Ménétrier, M.; Rougier, A.; Delmas, C. *Inorg. Chem.* **1995**, *34* (7), 1773−1778.
(10) Carlier, D.; Ménétrier, M.; Grey, C. P.; Delmas, C.; Ceder, G. *Phys. Rev. B* **2003**, *67*, 174103 1−14.

10.1021/cm070324n CCC: $37.00
Published on Web 07/25/2007

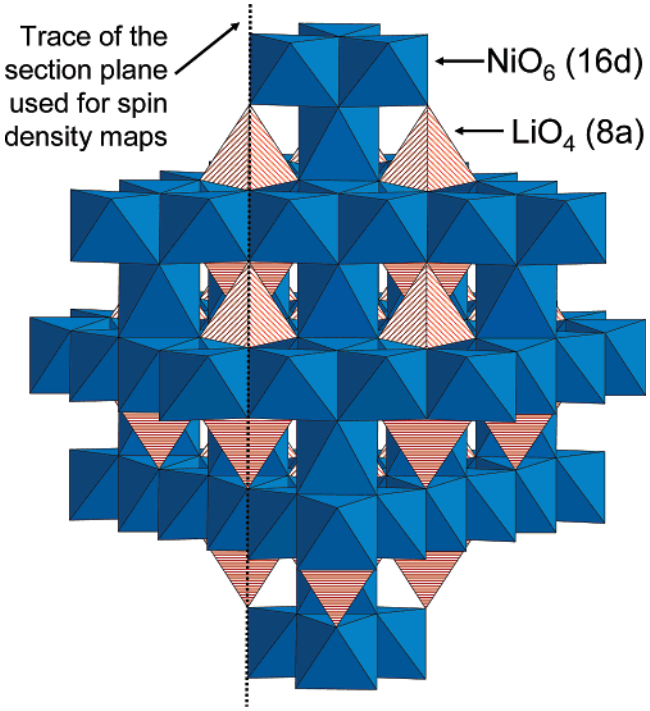

Figure 1. Representation of the spinel structure (*Fd*3*m* space group) where Li and Ni ions are located, respectively, in the 8a (tetrahedral) and 16d (octahedral) sites, oxygen atoms occupying the corners of the two polyhedra. The section plane used to show spin density maps in the following is perpendicular to the figure, with its trace shown as the vertical dotted line ((110) in *Fd*3*m* S.G.).

Table 1. Spin Density Transfer Mechanisms from t_{2g} and e_g* Single Electrons on a Transition Metal Ion to Li, when Both Occupy Edge-Sharing Octahedra Such as in the Layered Compounds; the Strength of the Interactions (in particular the 90° direct delocalization from nonbonding t_{2g}) Greatly Depends on the Nature of the Transition Element and the Distance from Li^+

Orbital with electron spin	Relative position of Li	Mechanism for transfer of electron spin density	Sign
t_{2g}	edge-sharing 90° Li-O-M	Direct delocalisation	Positive Strong
	corner-sharing 180° Li-O-M	Delocalisation from the polarised bonding e_g via oxygen	Negative Weak
e_g*	corner-sharing 180° Li-O-M	Delocalisation via oxygen	Positive Strong
	edge-sharing 90° Li-O-M	Direct delocalisation from polarised t_{2g} (if fully occupied)	Negative Weak

oxygen character, although the custom is often to refer to the former orbital as e_g.

In this table, the key role of the M−O−Li configuration is well-emphasized; for the MO_6 and LiO_6 coordination considered, the (nonbonding) t_{2g} orbital of M clearly points directly to the center of the edge-sharing octahedron containing Li, whereas the p orbitals of oxygen point toward the center of the two octahedra. They can therefore overlap with both the e_g* orbital of M and the s of Li.

Clearly, the situation is not so simple with other types of coordination, such as direct spinel type structures with a tetrahedral oxygen site for Li and an octahedral site for M, and an M−O−Li configuration close to 120° (Figure 1).

In such spinel compounds with Mn^{4+} (t_{2g}^3), Grey and coworkers have shown that the amount of electron spin transferred onto Li is intermediate between the 180° configuration (delocalization of weak negative spin density from polarized bonding e_g) and the 90° configuration (direct delocalization of strong positive spin density from t_{2g}) that one encounters in the Mn^{4+} layered compounds with octahedral Li coordination.[1] The nature of the spin transfer mechanism, however, was not discussed in the spinel case. In the pure Mn spinel $LiMn_2O_4$, where Mn is at the "3.5+" oxidation state (on the NMR time scale), it was shown that the Mn^{3+} character leads to a decrease in the Li NMR shift, which is also not obvious from the effects of Mn^{3+} ($t_{2g}^3e_g^1$) on octahedral Li. In this material, which is of great importance as the positive electrode of Li-ion batteries, additional NMR signals are also observed that are related to the actual stoichiometry of the compound, such as the presence of excess Li in the Mn site, leading to defects where some Mn ions are pinned to the 4+ oxidation state.[1]

To understand the nature of the spin transfer mechanisms in the spinel configuration, we have selected a cation with a simpler electronic configuration in the 3+ and 4+ states: Ni^{4+} is diamagnetic (t_{2g}^6, LS) whereas Ni^{3+} possesses one electron spin in the e_g* orbital ($t_{2g}^6e_g^1$, LS). The spinel $LiNi_2O_4$ compound is known to form when the partially deintercalated Li_xNiO_2 compounds are heated.[11−15] This is actually a key process in the thermal runaway of Li-ion nickel-containing batteries when exposed to abusive use leading to, for example, a short circuit, so understanding this structural transformation is quite important for mastering the safety of such batteries.[16,17] We report DFT calculations to model the spin density transfer mechanisms in the ideal $LiNi_2O_4$ spinel and a ^{7}Li NMR study of the formation of real spinel $LiNi_2O_4$ samples upon thermal treatment of electrochemically deintercalated Li_xNiO_2 close to $x = 0.5$.

Experimental Section

The starting materials $Li_{1-z}Ni_{1+z}O_2$ were obtained by the coprecipitation route described elsewhere.[2] Refinement of XRD data using the Rietveld method showed that $z = 0.007(5)$, 0.009(4), and 0.013(3) for the starting samples utilized.

The deintercalated phases, which we will call Li_xNiO_2 whatever z, were obtained by electrochemical deintercalation of the lithium nickelate phase using Li/$LiPF_6$ 1 M in 1:1:3 PC:EC:DMC/$Li_{1-z}Ni_{1+z}O_2$ cells. The positive electrode consisted of a $Li_{1-z}Ni_{1+z}O_2$/(1:1 carbon:graphite) (10−90 wt %) mixture or a pressed pellet (8

(11) Thomas, M. G. S. R.; David, W. I. F.; Goodenough, J. B.; Groves, P. *Mater. Res. Bull.* **1985**, *20*, 1137−1146.
(12) Kanno, R.; Kubo, H.; Kawamoto, Y.; Kamiyama, T.; Izumi, F.; Takeda, Y.; Takano, M. *J. Solid State Chem.* **1994**, *110*, 216−225.
(13) Dahn, J. R.; Fuller, E. W.; Obrovac, M.; Von Sacken, U. *Solid State Ionics* **1994**, *69*, 265−270.
(14) Arai, H.; Okada, S.; Sakurai, Y.; Yamaki, J. *Solid State Ionics* **1998**, *109*, 295−302.
(15) Lee, K.-K.; Yoon, W.-S.; Kim, K.-B.; Lee, K.-Y.; Hong, S.-T. *J. Power Sources* **2001**, *321*, 97−98.
(16) Guilmard, M.; Croguennec, L.; Denux, D.; Delmas, C. *Chem. Mater.* **2003**, *15*, 4476−4483.
(17) Guilmard, M.; Croguennec, L.; Delmas, C. *Chem. Mater.* **2003**, *15*, 4484−4493.

Table 2. Experimental Conditions Used for the Transformation of the Lithium Nickelate into the Spinel Phase via the Deintercalated Materials (P, pellet; M, $Li_{1-z}Ni_{1+z}O_2$/(1:1 carbon:graphite) Mixture)

z in $Li_{1-z}Ni_{1+z}O_2$	Li_xNiO_2		Heating temperature for the spinel transformation
	Electrode Technology	x	
0.007	P	0.53	210°C ≤ T ≤ 265°C
	P	0.53	210°C, 215°C, 220°C
0.009	M	0.52	120°C ≤ T ≤ 260°C
		0.52	220°C
		0.51	220°C
		0.48	210°C ≤ T ≤ 250°C
0.013	M	0.47	220°C

mm in diameter, 800 MPa) of pure material depending on the sample. The cells were charged at room temperature with a *C*/300 rate for pressed electrodes and a *C*/200 rate for carbon-mixed electrodes using alternate periods of open circuit relaxation. The voltage stability criterion for the relaxation periods was fixed at 1 mV/h. Various deintercalated phases exhibiting different deintercalation rates were prepared to be transformed into spinels. The positive electrodes were recovered at $0.47 \leq x \leq 0.53$ after being relaxed, washed with DMC, and vacuum-dried in an argon-filled glove box. The final open circuit voltage of these materials is in good agreement with the electrochemical cycling curve of $LiNiO_2$.[18]

Spinel phases were obtained after heating the deintercalated phases at various temperatures under an argon stream for 3 h. The increasing temperature slope was 2 °C/min. and the final material was air-quenched. In some cases, the sample was kept in the zirconia NMR rotor for the heating process, after removing the cap.

Table 2 summarizes the various operating conditions used for transformation of lithium nickelates into the spinel phase via the deintercalated materials.

X-ray diffraction patterns of selected spinel phases synthesized were recorded using a Siemens D5000 powder diffractometer with Cu−Kα radiation and a graphite diffracted beam monochromator. Since the spinel phases are hygroscopic, the XRD samples were prepared in an argon-filled glove box using airtight sample holders. For full pattern matching refinement, data were collected in the 5−120° (2θ) range in steps of 0.02° (2θ) with a constant counting time of 40 s. Refinement of the X-ray diffraction data was achieved using the full pattern matching method (FULLPROF program[19]).

The electronic conductivity measurements were carried out on an unsintered $LiNi_2O_4$ pellet, using the four-probe method with direct current in the 140−400 K range.

^{7}Li MAS NMR spectra were recorded on a Bruker 300 Avance spectrometer at 116 MHz (7.05 T magnet), with a standard 4 mm Bruker MAS probe. The samples were mixed with dry silica in order to facilitate spinning and to improve the field homogeneity, because they may exhibit metallic or paramagnetic properties. The mixture was placed into a 4 mm diameter zirconia rotor in the dry box. A combination of single pulse and Hahn echo sequences was used in MAS conditions (15 kHz spinning speed) for all phases. The single pulse sequence with $t_{\pi/2} = 2.4$ μs requires a first-order phasing process with a sin *x*/*x* baseline correction due to the dead time of the spectrometer. The Hahn echo sequence [$t_{\pi/2}-\tau_1-t_\pi-\tau_2$] was used to facilitate the phasing of all the signals and ensure the observation of possible very wide signals that are lost during the receiver dead time, while refocusing the interactions with electron spins.[2] The 90° pulse duration was equal to $t_{\pi/2} = 2.4$ μs. Variable-temperature (VT) NMR experiments were also carried out in the 295−400 K range using a Bruker WVT MAS probe.

Table 3. Optimized Structural Parameters for the $LiNi_2O_4$ Spinel Used for Spin Density Calculations[a]

atom	site	*x*	*y*	*z*
Li	8a	0.125	0.125	0.125
Ni	16d	0.5	0.5	0.5
O	32e	0.2622	0.2622	0.2622

[a] Space group = *Fdm*3; $a = 8.074$ Å.

First-principles calculations were performed using density functional theory (DFT) in the generalized gradient approximation (GGA) with the pseudopotential method as implemented in the Vienna ab initio Simulation Package (VASP).[20] A plane wave basis set with a cutoff energy of 400 eV was chosen. The reciprocal space sampling was performed with a k-point grid of 10*10*10 phase using an $Li_2Ni_4O_8$ cell (the primitive cell for the $LiNi_2O_4$ stoichiometric spinel). The structure was relaxed and the final energy of the optimized geometry was recalculated so as to correct for the changes in basis during relaxation. In our calculations, the spins of the transition metal ions are assumed to be aligned with the applied magnetic field at 0 K. To evaluate the amount and polarization of spin on the lithium and nickel nuclei, the polarized spin density was integrated in a sphere around each nucleus. Further details on the method used can be found elsewhere.[10]

Spin Density Calculations

In this section, we give and discuss the results of the spin density calculations and then describe the experimental results (NMR, XRD, and conductivity measurements) in the following section. These will be discussed in light of the calculations.

The spinel structure is illustrated in Figure 1, which will be referred to throughout the text.

Table 3 shows the structural parameters after the geometrical optimization step (although calculations were performed using the primitive $Li_2Ni_4O_8$ cell, the table uses the more classical cubic *Fd*3*m* cell).

Figure 2a shows the integrated amount of electron spin with positive polarization on the Ni nuclei. As expected by symmetry, only one type of Ni is identified, which carries a spin density close to 0.4 as shown by the plateau corresponding to a sphere of around one Å radius. Considering the partial oxygen character of the e_g* orbital (covalency), such a value is in very good agreement with the 0.5 electron spin expected for Ni ions with an average "3.5+" valence in a low-spin configuration (the low-spin electronic configuration for the calculated electronic structure is clearly apparent in the analysis of the density of states, not shown here). Note that calculations were made with this $Li_2Ni_4O_8$ cell as well as with larger cells with slight distortions in their input position to make the Ni atoms symmetrically nonequivalent, but also led to identical Ni ions. However, it is

(18) Croguennec, L.; Pouillerie, C.; Delmas, C. *J. Electrochem. Soc.* **2000**, *147* (4), 1314.
(19) Rodriguez-Carvajal, J. *WinPLOTR: A Graphic Tool for Powder Diffraction Pattern Analysis*; Laboratoire Léon Brillouin: Saclay, France, 2004; http://www-llb.cea.fr/fullweb/powder.htm.
(20) Kresse, G.; Furthmuller, J. *Comput. Mater. Sci.* **1996**, *6*, 15.

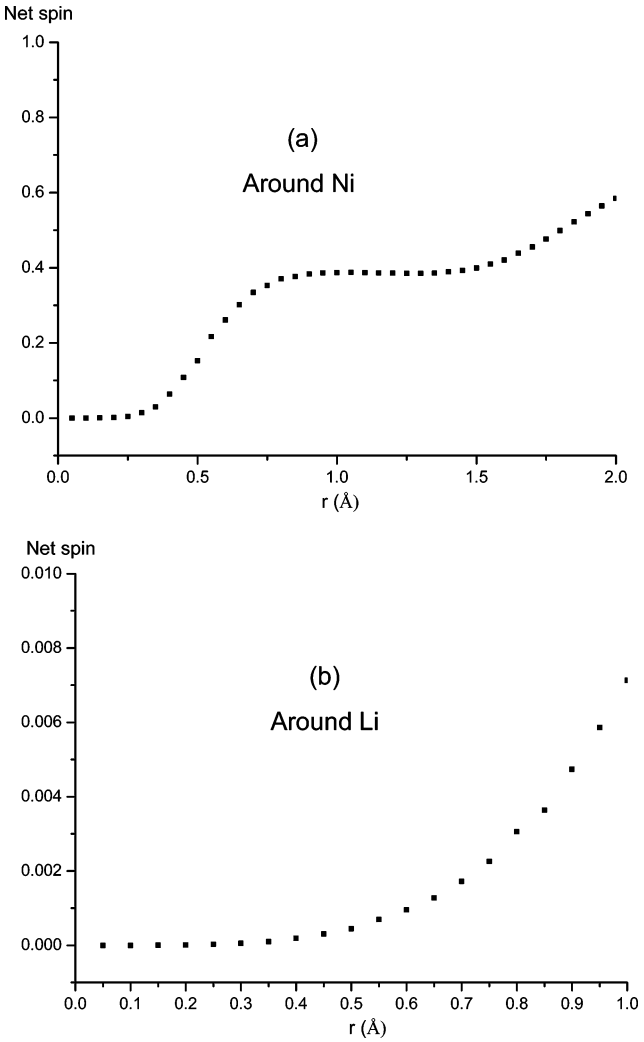

Figure 2. Integrated net spin in spheres with various *r* radii around the (a) Ni and (b) Li nuclei as a result of the DFT calculation for $LiNi_2O_4$.

known that with the approximation used, DFT does not tend to localize the charges in such compounds.[21]

Figure 2b gives the net spin integration around Li, and shows that a positive spin density is transferred onto Li. From previous calculations by some of us, a very rough estimation of the NMR shift expected on that basis can be given; indeed, considering a 0.8 Å radius sphere as representative of the electron spin density present at the location of the Li nucleus, the ratio between the calculated net spin on Li and the experimental RT Li NMR shift was found to be identical for both Li in the 180° Li−O−Ni configuration with one Ni^{3+} in Li(Ni,Co)O_2 (0.8×10^{-3} spin; +110 ppm) and $LiNiO_2$ (5.3×10^{-3} spin; +720 ppm).[10] Considering the same ratio for the spinel, the calculated net spin in a 0.8 Å sphere around Li of 2.8×10^{-3} (Figure 2b) would correspond to a contact shift of approximately 380 ppm. This approximation actually assumes that the fraction of polarized spin on the Ni ion at RT vs the one considered at 0 K (i.e., all the electron spins aligned with the applied field) is the same for the different compounds (paramagnetic behavior).

Figure 3a shows a section of the spin density map in the (110) plane of the *Fd*3*m* spinel structure, as shown in Figure 1. This plane contains Ni and Li atoms (Figure 3b); however, the oxygen atoms are not strictly contained in this plane, but very close. The map clearly shows the electron spin density polarized positively in the two lobes of the e_g* orbitals of Ni pointing toward oxygen, as expected in octahedral coordination. Actually, a portion of other lobes belonging either to the same or to other e_g* orbitals can also be seen, although they do not fully belong to the section plane. What is more interesting is the oxygen situation. Its environment is a rather elongated $LiNi_3$ triangular pyramid (Ni−Ni edge distance, 2.85 Å; Ni−Li edge distance, 3.35 Å), with very similar O−Li (1.91 Å) and O−Ni (1.93 Å) bond lengths; therefore, the oxygen orbitals of interest are not the same as in the layered case, where O is also octahedrally coordinated by Li and the transition metal ion. Thus, the orbitals on O point neither exactly toward Ni nor toward Li. However, the important fact is that there is still a significant overlap with the e_g* orbital on Ni, so that a positive electron spin density can be transferred to the Li site. The mechanism involved here is therefore clearly a delocalization via oxygen (see Table 1), although the orbitals on oxygen are not ideally oriented for it. Each Li nucleus thus receives a positive electron spin density from twelve Ni ions with a 122° Li−O−Ni configuration, with an average "3.5+" oxidation state. In such a configuration, each Ni^{3+} ion transfers 0.47×10^{-3} electron spin on Li (one-sixth of 2.8×10^{-3} net spin in the 0.8 Å radius sphere), which is a little bit more than half the spin density it transfers in the 180° configuration in the layered Ni,Co compound (0.8×10^{-3}) where the oxygen orbitals are ideally oriented.

Experimental Results

Figure 4 shows the ^{7}Li MAS NMR spectra along the progressive transformation of $Li_{0.52}NiO_2$ into the spinel phase and its decomposition. Each spectrum was recorded at RT after the thermal treatment indicated on the figure, using both a single-pulse (a) and a Hahn echo (b) pulse sequence.

In addition to the signals of interest discussed below, a signal at 0 ppm with its spinning sidebands set is always observed. This originates from Li in the solid electrolyte interphase (SEI) created by reaction with the electrolyte in the electrochemical cell, a complex mixture of mostly organic and mineral carbonates at the surface of the electrode material.[22]

For the pristine layered $Li_{0.52}NiO_2$ with *C*2/*m* space group, a rather broad signal at around 525 ppm, still separated into spinning sidebands, is observed by using a single-pulse experiment, whereas its intensity is significantly reduced in the Hahn echo spectrum. As discussed in detail in a previous paper, heating restored the observation of the echo signal, which was considered to correspond to Li undergoing a slow exchange due to correlated Li/vacancy and Ni^{3+}/Ni^{4+} hopping at room temperature, inducing a movement in the time scale of the Hahn echo sequence, i.e., 133 μs for evolution plus refocussing period prevents the echo formation.[23] For samples

(21) Zhou, F.; Cococcioni, M.; Marianetti, C. A.; Morgan, D.; Ceder, G. *Phys. Rev. B* **2004**, *70*, 235121.

(22) Ménétrier, M.; Vaysse, C.; Croguennec, L.; Delmas, C.; Jordy, C.; Bonhomme, F.; Biensan, P. *Electrochem. Solid-State Lett.* **2004**, *7*, A140−A143.

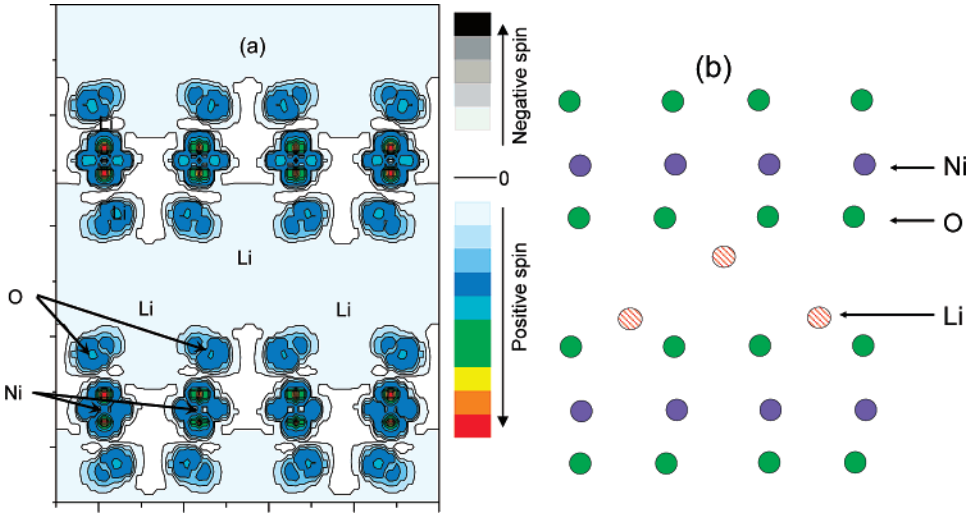

Figure 3. (a) Spin density map as a result of the DFT calculation for $LiNi_2O_4$ in a section plane with atom positions shown in (b). The position of this section plane in the spinel structure is shown in Figure 1.

having undergone the first steps of the progressive thermal treatment (120−160 °C), this signal vanishes and is replaced by a new signal growing at around 50 ppm, observed both in single-pulse and echo modes, suggesting either absence of movement (which we consider highly unlikely because of the nature of the compound) or a faster hopping (longer apparent T2 relaxation time, allowing the echo refocusing process at room temperature). The latter signal then grows while shifting to higher parts per million values and broadening after the 160−180 °C treatments, still with full echo observation. In the 180−220 °C range, this broadened signal is progressively replaced by a set of three signals at 265, 305, and 350 ppm with their respective spinning sidebands (see further, Figure 7), which are also observed in echo, with a change in their relative ratio when the thermal treatment temperature increases. Finally, after treatments to 240 °C and above, these signals in turn disappear and are replaced by a very broad signal, not separated into spinning sidebands.

Simultaneously, the magnitude of the 0 ppm signal progressively decreases, suggesting that the SEI might disappear after the thermal treatments, which is not unexpected for an organic surface layer.

XRD analysis of some of the thermally treated samples shows that (i) the *C*2/*m* pristine compound gradually transforms into an $R\bar{3}m$ one in the first steps of the thermal treatment and (ii) a phase with the spinel *Fd*3*m* symmetry is present in the temperature range 200−230 °C, in agreement with Guilmard et al.[16,17] However, the diffractogram of these spinel phases, such as that shown in Figure 5a for a representative sample, do not show a uniform angular variation of the full width at half-maximum, suggesting the presence of strains and/or defects in these samples. A Pseudo-Voigt profile function allows the experimental global intensity of the XRD pattern to be accounted for, but for most of the lines, the calculated full width at half-maximum is significantly different from the experimental one, either too large or too small (not shown). Figure 5b shows the example of a material just before the spinel transformation is complete, with a remaining $R\bar{3}m$ phase also detected.[16,17] The broad feature observed at about 20° on the X-ray diffractogram is due to the amorphous silica used in the mixture for NMR experiments. The corresponding NMR spectrum (Figure 6) shows both the broad signal and the appearance of the set of three signals mentioned above and shown in more detail in the following paragraph, in addition to the 0 ppm SEI signal with its spinning sidebands.

Several Li_xNiO_2 phases were prepared with compositions ranging from 0.47 to 0.53 from different $Li_{1+z}Ni_{1-z}O_2$ precursors and heat-treated in the 200−250 °C range. The corresponding NMR spectra consistently show a set of three signals, with their spinning sidebands (in addition to the 0 ppm signal and its spinning sidebands) as detailed in Figure 7 as an example. When various temperatures were used for a given sample in the 200−230 °C range, a change in the relative ratio of the three signals was observed, as is apparent in Figure 4 as an example. When considering the NMR spectra of various spinel phases obtained following the conditions given in Table 2, one can notice fluctuations (10−20°) in the temperature where the spinel phase forms and in the relative ratio of the three signals, but we could not establish a correlation between these features and the actual stoichiometry of the spinel phase, nor with the actual Ni content of the starting $LiNiO_2$ (see the Supporting Information). There are also fluctuations in the magnitude of the 0 ppm SEI signal depending on the electrochemical cell technology and probably the washing efficiency when recovering the layered $Li_{\sim 0.5}NiO_2$ material. This can hinder observation of the signals from the spinel due to overlap with one spinning sideband of the 0 ppm signal.

Electronic conductivity measurement of the spinel phase reported in Figure 8 and Table 4 shows significantly higher conductivity and lower activation energy than for the layered $Li_{0.53}NiO_2$ phase for which we concluded that ion and electron hopping are coupled to each other at the atomic scale on the basis of variable temperature ^{7}Li experiments.[23]

(23) Chazel, C.; Ménétrier, M.; Croguennec, L.; Delmas, C. *Inorg. Chem.* **2006**, *45*, 1184−1191.

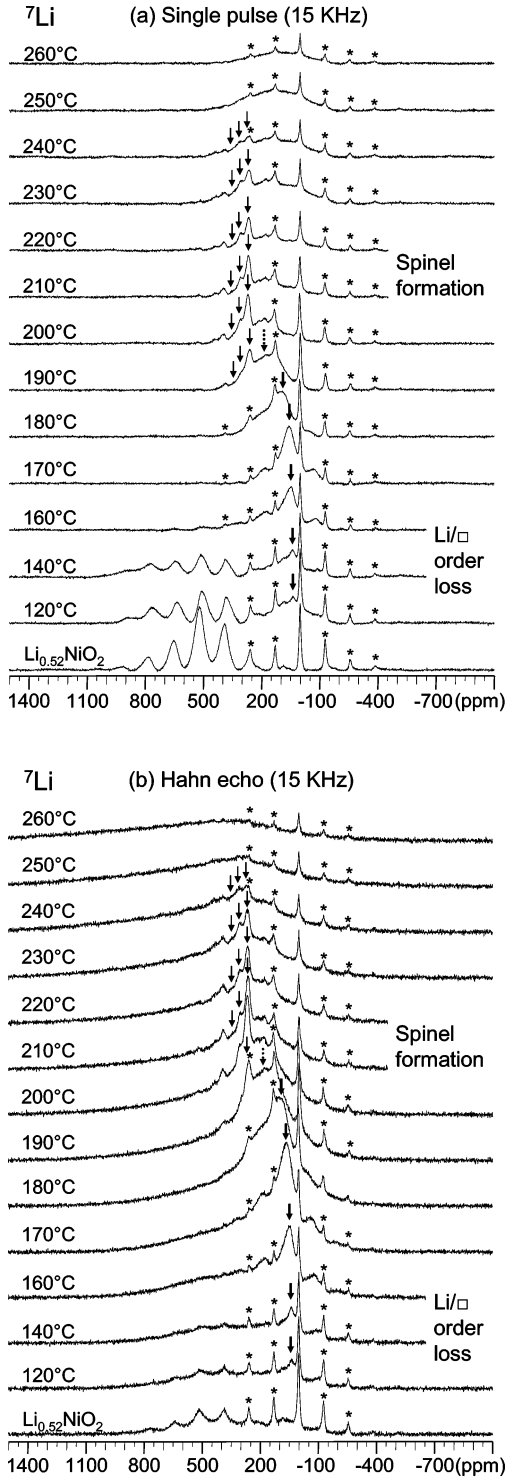

Figure 4. Room-temperature ^{7}Li MAS NMR spectra of the $Li_{0.52}NiO_2$ layered compound and after heat treatment up to 260 °C: (a) single pulse; (b) Hahn echo. Spinning speed is 15 kHz. Spinning sidebands of the 0 ppm signal are shown by *. Arrows show the new signals appearing upon heating (isotropic position). The spectra are plotted in a normalized intensity scale.

Discussion

Guilmard et al. have discussed the possible mechanisms for transformation of the layered $Li_{0.5}NiO_2$ into the spinel $LiNi_2O_4$ on the basis of diffraction data.[16,17] During thermal treatment in the 110−200 °C range, the monoclinic distortion of $Li_{0.5}NiO_2$ disappears, leading to an $R\bar{3}m$ phase. In a first step, the Li/vacancy ordering was thus considered to disappear, and Ni ions then start to migrate to the Li layer. In the corresponding NMR spectra (Figure 4), this indeed suppresses the 525 ppm signal that we assigned to a local Li/vacancy and Ni^{3+}/Ni^{4+} ordering in a previous paper.[23] This is complete at 170 °C. As mentioned above, a signal displaying the characteristics expected for mobile ions partially replaces it, which is in good agreement with the vacancies now also present in the transition metal layers and with the absence of tendency for any local ordering. It is meaningless to discuss its contact shift because the whole intensity of the original signal is obviously not recovered, particularly in the 160−200 °C range, which means that many Li ions with a very large distribution of environments in terms of Ni ions are not clearly observed, probably because they do not lead to a well-defined signal. This signal drastically changes in the temperature range corresponding to the Ni migration process and arises from a rather broad distribution of environments just before the spinel formation. This is illustrated by Figure 5b, where the *Fd*3*m* and the $R\bar{3}m$ phase are identified by XRD, and Figure 6, where NMR

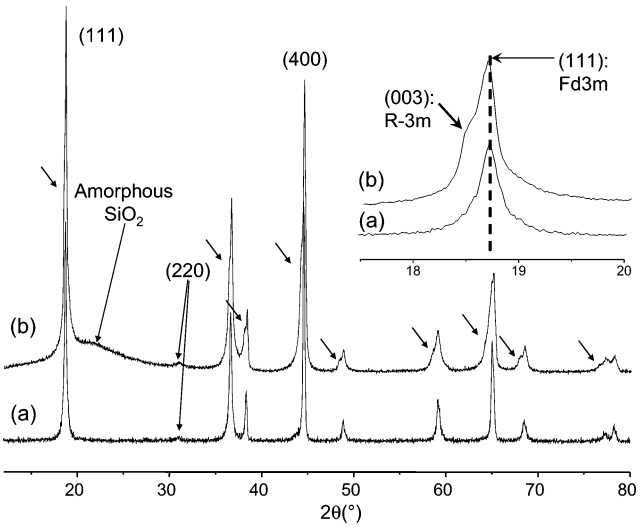

Figure 5. X-ray diffractograms for (a) the $Li_{0.53}NiO_2$ spinel compound heated at (a) 210 °C and (b) $Li_{0.48}NiO_2$ spinel compound heated at 210 °C (arrows show the lines due to the remaining layered phase).

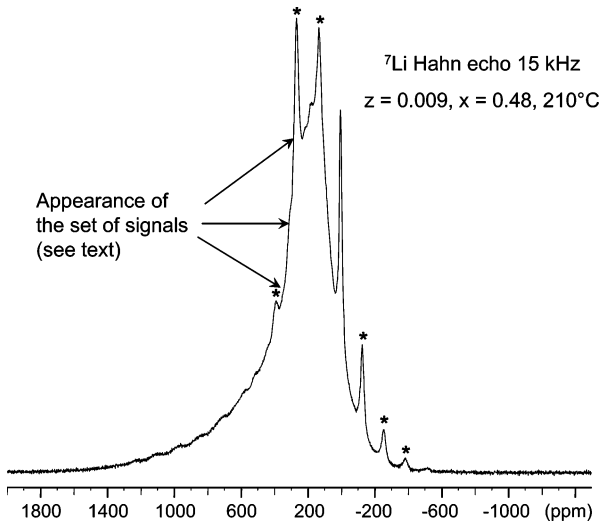

Figure 6. ^{7}Li MAS NMR spectrum for the $Li_{0.48}NiO_2$ spinel compound heated at 210 °C (Hahn echo, 15 kHz, * = spinning sidebands of the 0 ppm signal).

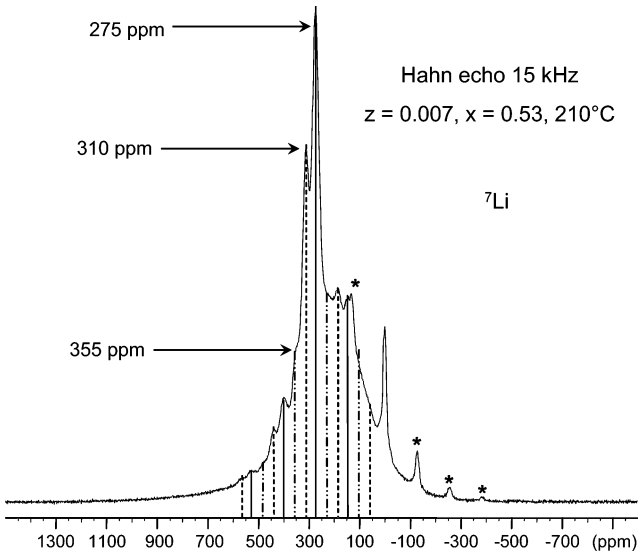

Figure 7. ^{7}Li MAS NMR spectrum for the $Li_{0.53}NiO_2$ spinel compound heated at 210 °C (Hahn echo, 15 kHz). The isotropic signals are shown by arrows, their spinning sidebands are shown by sets of vertical lines, and by * for the 0 ppm SEI signal.

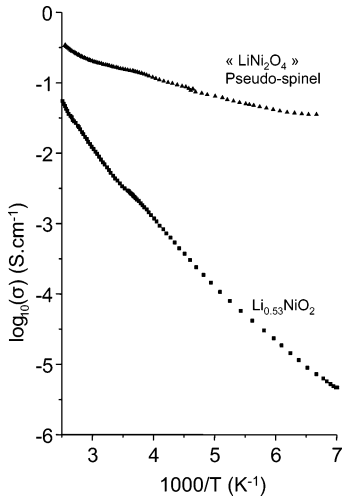

Figure 8. Electronic conductivity (dc four probe method with unsintered pellets) for $Li_{0.53}NiO_2$ and the spinel phase obtained after heating the latter to 210 °C.

Table 4. Electronic Conductivity Results for the Spinel $LiNi_2O_4$ Phase, as Compared to Those of the Pristine Layered $Li_{0.53}NiO_2$ One

	log σ (S cm^{-1}) at R.T.	E_a (eV)	T range (K)
layered $Li_{0.53}NiO_2$	−2.32	0.25	295−395
pseudo spinel	−0.77	0.05	160−340

shows both this broad signal and the ones assigned to the spinel phase (see below).

When more and more Ni ions move to the (formerly) Li layer, the latter start to occupy the tetrahedral sites, which are favorable because they now share a face with vacancies in the (formerly) transition metal layer. This corresponds to the formation of the spinel-type phase, which was called "pseudo-spinel", considering that its ordering was not perfect.[16,17]

In a perfect spinel, as confirmed by our calculations, one would expect a single NMR signal for Li in the tetrahedral 8a site, estimated by our calculations to be around 380 ppm. As in the case of the $LiMn_2O_4$ spinel,[1] this signal is expected to result from an exchange due to fast electronic Ni^{3+}/Ni^{4+} hopping so that it should also be observed in echo conditions (long T2), as inferred from the high electronic conductivity value measured for the $LiNi_2O_4$ spinel (Figure 8 and Table 4).

Our experimental NMR observation is rather a set of three signals (Figures 7), with a good echo observation, at 265, 305 and 350 ppm, which suggests well-defined Li environments in the spinel compound. On the basis of our calculations described above, this is not compatible with a stoichiometric spinel material. Besides, the high conductivity value reported above suggests that fast Ni^{3+}/Ni^{4+} hopping in the NMR time scale could lead to an identical average effective charge for all the Ni ions. The NMR signals would then result from a fast exchange of the surrounding of Li (more precisely the electron spins on Ni that determine the contact shift in such compounds), in agreement with their echo observation. We have carried out variable-temperature NMR measurements up to 400 K for a spinel material, showing a slight decrease in the separation between the three signals, but definitely no conclusive sign of exchange between these signals. In addition, the echo observability of the signals remains at elevated temperatures, suggesting that no ionic exchange process starts to occur. This is consistent with the picture of signals resulting from different sites in the material, with no ionic exchange between them, each signal resulting from an electronic exchange of their surrounding.

Several types of defects are possible as a result of the layered to spinel transformation, as discussed by Guilmard et al.[16,17] and by Reed et al. in the manganese case.[24,25] In particular, migration of the transition metal ion from the layer to the interlayer octahedral sites proceeds through a tetrahedral site, the partial occupation of which was found energetically favorable in the case of Mn, leading to a partially inverse spinel with some Li ions still in octahedral sites and some Mn^{2+} ions in tetrahedral sites, resulting from partial disproportionation of Mn^{3+}.[24,25] With no ordering, such a structure should also lead to an *Fd*3*m* type XRD pattern. In the case of Ni, Ni^{3+} (in the high spin state) could also be somewhat stable in tetrahedral coordination,[16,17] and one could also envisage a disproportionation into Ni^{2+} and Ni^{4+}. Such situations could cause a pinning of the charges of Ni in defect sites, and create specific environments for the nearby Li ions, with transferred electron spin density that we are not able to model at this point. Further work is in progress to investigate what type of defect is most likely at the origin of the complex but well-defined NMR pattern observed.

As concerns the final part of the thermal treatment, the disappearance of the "spinel" NMR signals corresponds to temperatures at which the formation of a new $R\bar{3}m$ type phase was observed, corresponding to the beginning of decomposition of the material with oxygen evolution, and possibly Li loss.[16,17] This is clearly not complete at the temperatures explored in the present work, but this must lead to a very broad distribution of Li environments in terms of transition

(24) Reed, J.; Ceder, G.; Van Der Ven, A. *Electrochem. Solid-State Lett.* **2001**, *4*, A78.
(25) Reed, J.; Ceder, G. *Chem. Rev.* **2004**, *104*, 4513−4533.

metal including Ni^{2+}, which will increase the dipolar part of the interaction, possibly leading to the very broad signal observed.

Conclusion

Our DFT calculations in the spinel $LiNi_2O_4$ have shown that the electron spin density transfer mechanism from octahedral Ni^{3+} ions ($t_{2g}^6e_g^1$) to tetrahedral Li with close to 120° Li−O−Ni configuration is a delocalization type one, although the p orbitals on oxygen (with a pyramidal $LiNi_3$ environment) are not aligned with the e_g* orbital of Ni and the Li nucleus. Because of this misalignment, the amount of spin density transferred per Ni^{3+} ions is approximately half that transferred in the 180° Li−O−Ni configuration of layered compounds with octahedral environment for Li and Ni (and O) where the p orbital of oxygen is ideally oriented.

The ^{7}Li NMR signal consistently observed for spinel-type $LiNi_2O_4$ obtained by heat treatment of layered Li_xNiO_2 ($0.47 < x < 0.53$) is clearly different from the one expected for a stoichiometric $LiNi_2O_4$ spinel. A set of three signals is always observed with slight fluctuations in their relative magnitude with no apparent correlation with the actual composition of the spinel (x). This suggests that the spinel phase formed is far from the ideal structure and always exhibits the same kind of (so far unidentified) defect probably related to nonideal site occupancy by Li and Ni, following their migration mechanisms from their sites in the layered phase.

Acknowledgment. The authors thank G. Ceder for discussions and for providing calculation means, B. Delatouche for technical assistance, and Région Aquitaine (CPER Véhicule Electrique 21-13) for financial support of NMR equipment.

Supporting Information Available: ^{7}Li MAS NMR spectra for various spinel compounds originating from $Li_{(1-z)}Ni_{(1-z)}O_2$ (PDF). This material is available free of charge via the Internet at http://pubs.acs.org.

CM070324N